2018 26th Mediterranean Conference on Control and Automation (MED)
Zadar, Croatia, June 19-22, 2018

Modeling of the citric acid cycle and its two shuttle systems

Gergely Sváb[1,2], Gergő Horváth[1] and Gábor Szederkényi[2]

Abstract— **A dynamical model is proposed in this paper for describing the key quantities of mitochondrial metabolism. Mitochondria are very important cell organelles, because they take part in the bioenergetic functions of the cells, control metabolic pathways, participate in heat production, in upholding the equilibrium of reactive oxygen species, in Ca^{2+} metabolism, and in the control of apoptotic procedures of the cells. In this work the citric acid cycle and its two transport systems are modeled, namely the malate-aspartate and the citrate-pyruvate shuttle. The overall model containing three modules is given in the form of kinetic ordinary differential equations with 39 state variables. Simulation results are presented and discussed from a biological point of view.**

I. INTRODUCTION

In the Neurobiochemistry working group (Department of Medical Biochemistry, Semmelweis University), we have performed kinetic measurements of several mitochondrial enzymes, and we have determined and analyzed interactions between enzymes and substrates. We have measured reactive oxygen species productions and the mitochondrial O_2 consumptions with different respiratory substrates [1]–[4]. The need naturally arises for further analysis of the process. Therefore, a suitable quantitative (mathematical) model is constructed which describes the temporal changes in the quantities of citric acid cycle's molecules.

In previous studies similar models [5]–[8] were constructed. Therefore, we summarize the most relevant results below.

The first model [5] uses rapidly evolving equilibrium state which is determined by kinetic and thermodynamical equilibrium. The model contains many parameters that should be determined appropriately. The parameter values cover a wide range. This model can predict the individual factors and effects (NADH, ATP, metabolic fluxes) in the regulation of citric acid cycle function and projects the effect of pH and membrane potential changes on ATP synthesis.

The model published in [6] describes the simplified model of citric acid cycle, electron transport chain and ATP synthesis and their relations to each other. In this model the number of reaction equations is reduced significantly and mostly irreversible reactions are used instead of reversible reactions. Due to this the mathematical analysis becomes easier. Describing the reactions model the authors use differential equations which can show changes in concentrations during the simulated time. Additionally, this model takes in account the effect of membrane potential to the ATP synthesis.

The authors in [7] examine the process of the citric acid cycle, electron transport chain and ATP synthesis. Reactions of the citric acid cycle are described with 8 differential equations and Michaelis-Menten reaction kinetics. Dynamics of the electron transport chain and ATP synthesis are described by the difference of the concentrations and the pH. Moreover, the model examines the ATP synthesis, the function of O_2 concentration and intramitochondrial pH.

The model in [8] extends the earlier model [7] with two transporter systems, which are the malate-aspartate and citrate-pyruvate shuttles. These transporter systems transport the NADH molecules between the intermembrane space and mitochondrial matrix which regenerates the cytoplasmic NAD^+ pool. Additionally, because of the changing mechanism these shuttle systems can keep the equilibrium of the different number of carbon chains in the mitochondrial matrix.

The most important goal of our modeling is to describe the functions of the mitochondria in healthy and pathologic states with a dynamic system. We would like to test this model in different pathological conditions and compare our results with the physiological measurements. If the model is accepted, it could be used in simulations of modified metabolic status in various enzyme defects by modifying the parameters of examined enzymes. With this model, we plan to predict the altered metabolic state of the pathological status, and to get a forecast about the mitochondrion, which may either adapt to the modified metabolic status or it may show pathological functions, that can ultimately lead to the death of the mitochondrion.

II. BIOLOGICAL BACKGROUND

A. Process description

Mitochondria are cell organelles with prokaryotic origin that established endosymbiosis with ancient eukaryotic cells during evolution. Citric acid cycle is a complex enzyme system in mitochondria, and a key step of metabolism. Mitochondria produce energy during the catabolic degradation of carbohydrates, fats, proteins and nucleic acids. Additionally, molecules of the citric acid cycle take part as precursors in the construction of the anabolic procedures [9]. Molecules involved in the citric acid cycle can transform into each other depending on the current metabolic status of mitochondria.

This project was partially supported by the European Union, co-financed by the European Social Fund (EFOP-3.6.2-16-2017-00013 and EFOP-3.6.3-VEKOP-16-2017-00009).

[1]Department of Medical Biochemistry, Semmelweis University, Tűzoltó u. 37-47, H-1094 Budapest, Hungary gergely@svab.hu

[2]Faculty of Information Technology and Bionics, Pázmány Péter Catholic University, Práter u. 50/a, H-1083 Budapest, Hungary szederkenyi@itk.ppke.hu

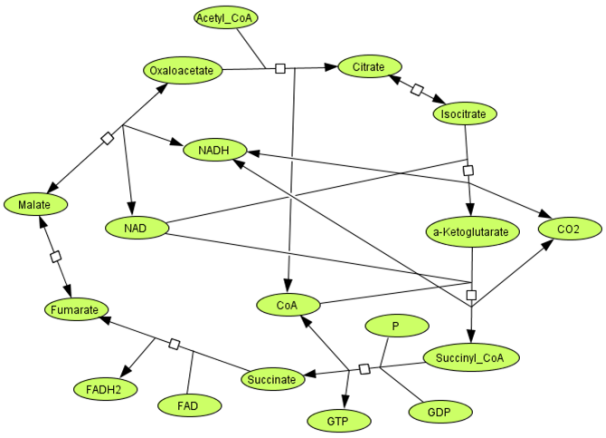

Fig. 1. Reaction graph of citric acid cycle

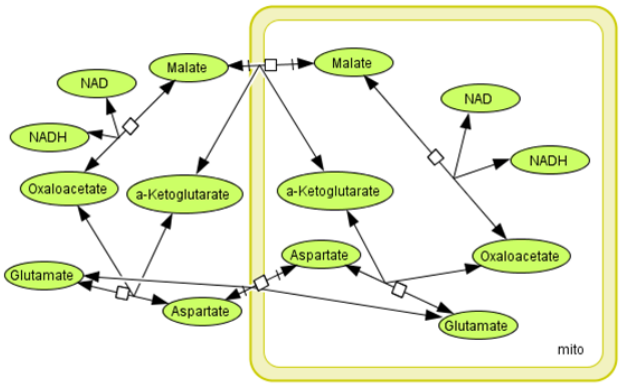

Fig. 2. Reaction graph of malate-aspartate shuttle

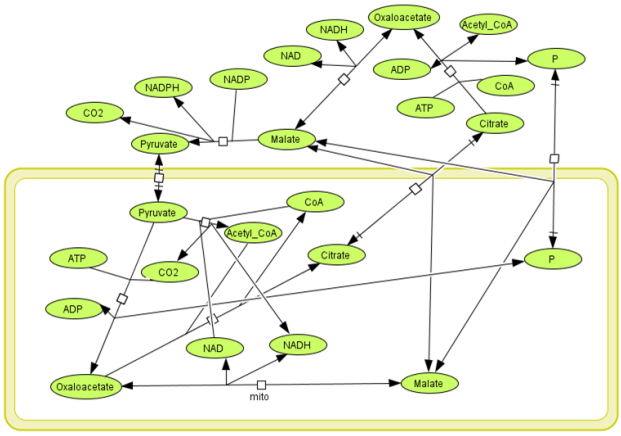

Fig. 3. Reaction graph of citrate-pyruvate shuttle

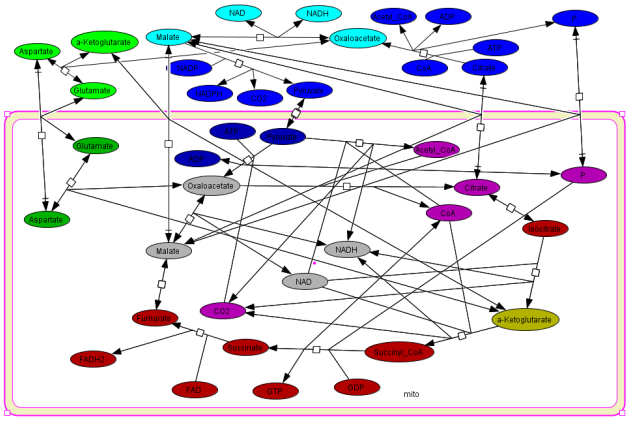

Fig. 4. Reaction graph of integrated model

B. The modeled reactions

In this work we modeled the reaction network of citric acid cycle (CAC, Fig. 1), malate-aspartate shuttle (MAS, Fig. 2) and citrate-pyruvate shuttle (CPS, Fig. 3). In the first step we construct 3 individual modules for each process, and after that we combine them to an integrated model (Fig. 4).

The following list contains the reactions corresponding to the different modules and their catalyzing enzymes/transporters involved in our model. The format of the description is: Number of reaction: name of enzyme (Abbreviation of enzyme, Enzyme Commission (EC) number of enzyme). Note that reversible reactions are modeled as two elementary reaction steps. Furthermore, there are reactions which are present in more than one module.

Module 1: Reactions of citric acid cycle

R1.1: Citrate synthase (CS, 4.1.3.7):
$Acetyl\text{-}CoA\ (AcCoA) + oxaloacetate\ (OA) \rightarrow citrate\ (Cit) + CoA\text{-}SH\ (CoA)$

R1.2, R1.3: Aconitase (ACON, 4.2.1.3):
$Cit \rightleftharpoons isocitrate\ (ICit)$

R1.4: Isocitrate dehydrogenase (IDH, 1.1.1.41):
$ICit + NAD^+ \rightarrow \alpha\text{-}ketoglutarate\ (\alpha KG) + CO_2 + NADH + H^+$

R1.5: α-ketoglutarate dehydrogenase (αKGDH, 1.2.4.2):
$\alpha KG + CoA + NAD^+ \rightarrow succinyl\text{-}CoA\ (SucCoA) + CO_2 + NADH + H^+$

R1.6: Succinyl-Coenzyme A ligase (SCS, 6.2.1.4):
$SucCoA + GDP + H_2PO_4^-\ (P) \rightarrow succinate\ (Suc) + CoA + GTP$

R1.7: Succinate dehydrogenase (SDH, 1.3.5.1):
$Suc + FAD \rightarrow fumarate\ (Fum) + FADH_2$

R1.8, R1.9: Fumarate hydratase (FH, 4.2.1.2):
$Fum + H_2O \rightleftharpoons malate\ (Mal)$

R1.10, R1.11: Malate dehydrogenase mitochondrial (MDH-m, 1.1.1.37):
$Mal + NAD^+ \rightleftharpoons OA + NADH + H^+$

Module 2: Reactions of malate-aspartate shuttle
R2.1, R2.2: Malate dehydrogenase extramitochondrial (MDH-c, 1.1.1.37):
$Mal + NAD^+ \rightleftharpoons OA + NADH + H^+$

R2.3, R2.4: Aspartate transaminase mitochondrial (ASAT-m, 2.6.1.1):
$Aspartate\ (Asp) + \alpha KG \rightleftharpoons OA + glutamate\ (Glu)$

R2.5, R2.6: Aspartate transaminase extramitochondrial (ASAT-c, 2.6.1.1):
$Asp + \alpha KG \rightleftharpoons OA + Glu$

R2.7, R2.8: α-ketoglutarate transporter (αKGT):
$\alpha KG \rightleftharpoons Mal$

R2.9, R2.10: Aspartate-glutamate carrier (AGC):
$Asp \rightleftharpoons Glu$

Additionally Module 2 contains R1.10 and R1.11.

Module 3: Reactions of citrate-pyruvate shuttle
R3.1: ATP citrate synthase (ACS, 4.1.3.7):
$Cit + CoA + ATP \rightarrow OA + AcCoA + ADP + P$

R3.2: Malic enzyme mitochondrial (ME-m, 1.1.1.40):
$Mal + NAD^+ \rightarrow pyruvate\ (Pyr) + NADH + H^+ + CO_2$

R3.3: Malic enzyme extramitochondrial (ME-c, 1.1.1.40):
$Mal + NADP^+ \rightarrow Pyr + NADPH + H^+ + CO_2$

R3.4: Pyruvate dehydrogenase (PDH, 1.2.4.1):
$Pyr + CoA + NAD^+ \rightarrow AcCoA + NADH + H^+ + CO_2$

R3.5: Pyruvate carboxylase (PC, 6.4.1.1):
$Pyr + CO_2 + ATP \rightarrow OA + ADP + P$

R3.6, R3.7: Citrate transporter (CTP):
$Cit + H^+ \rightleftharpoons Mal$

R3.8, R3.9: Dicarboxylate carrier (DIC):
$Mal \rightleftharpoons P$

R3.10, R3.11: Pyruvate transporter (PT):
$Pyruvate \rightleftharpoons pyruvate$

Additionally Module 3 contains R1.1, R1.10, R1.11, R2.1 and R2.2.

III. Kinetic model

A. Modeling goals

Our model simulates reactions of the citric acid cycle and its two transport systems. The goals of the work were the following:

1) To determine the set of substrates which participate in the key mechanisms of the system.
2) To model transporter mechanisms.
3) To integrate the transporter processes with the mode of the mitochondrial metabolism.

Reaction rates in our model cycle were described by Michaelis-Menten kinetics. Reversible reactions were described as two opposite elementary reaction steps. The changes of intermediates were described by differential equations.

B. The applied kinetics

Assuming Michaelis-Menten kinetics, the general form of the reaction rates is

$$V([S],E) = \frac{V_{max}(E)\cdot[S]}{K_m(E,S)+[S]} \quad (1)$$

where the V([S],E) is the reaction rate which depends on the substrate concentration and enzyme, [S] is the concentration of the substrate, V_{max}(E) is the maximum reaction rate of enzyme E, and K_m(S,E) is the Michaelis-Menten constant, which represent the enzyme substrate affinity. Reaction rates of transport processes (R2.7 – R2.10, R3.6 – R3.11) were determined using the approach described in [10].

IV. Description of the reactions

A. Reaction rates

The rates of first order reactions were assumed in the form of Eq. (1).

Based on [7], the rates of higher order reactions of the form

$$S_1 + S_2 + \ldots + S_n \rightarrow P_1 + P_2 + \ldots + P_l$$

are described as

$$V([S_1],\ldots,[S_n],E) = V_{max}(E)\cdot\frac{[S_1]}{[S_1]+K_m(S_1,E)}\cdot\ldots\cdot\frac{[S_n]}{[S_n]+K_m(S_n,E)},$$

where $V_{max}(E)$ and $K_m(S_i,E)$ for $i = 1,\ldots,n$ are kinetic constants depending on the enzyme and the substrates.

B. Dynamical model

The ODEs of the model are in the following standard form

$$\dot{X}(t) = \Sigma\cdot\bar{V}(X(t)),$$

where $X(t) \in \mathbb{R}^n$ is the concentration vector given in Table I (where (m) and (c) denotes matrix and cytoplasmatic concentrations, respectively), $\Sigma \in \mathbb{R}^{n\times k}$ is the stoichiometric matrix (assuming k reactions), and $\bar{V}(X)$ is the vector of reaction rates. Note that Σ can be written from the list of reactions given in Section II.B.

Initially, we constructed and tested the sub-models of the different modules separately. During these preliminary tests, the input concentrations of the modules were constant physiological values. The brief description and the reaction rate vectors of the individual subsystems are given below.

Module 1: Citric acid cycle
In this module citric acid cycle (CAC) contains 8 enzymes. These enzymes catalyze 5 irreversible and 3 reversible reactions described by 18 differential equations. This module

X_n	Abbr		X_n	Abbr		X_n	Abbr
X_1	AcCoA (m)		X_{14}	AcCoA (c)		X_{27}	NAD^+ (m)
X_2	CoA (m)		X_{15}	CoA (c)		X_{28}	NADH (m)
X_3	OA (m)		X_{16}	OA (c)		X_{29}	NAD^+ (c)
X_4	Cit (m)		X_{17}	Cit (c)		X_{30}	NADH (c)
X_5	ICit		X_{18}	CO_2 (m)		X_{31}	$NADP^+$ (c)
X_6	αKG (m)		X_{19}	αKG (c)		X_{32}	NADPH (c)
X_7	SucCoA		X_{20}	ADP (m)		X_{33}	ADP (c)
X_8	Suc		X_{21}	ATP (m)		X_{34}	ATP (c)
X_9	Fum		X_{22}	P (m)		X_{35}	P (c)
X_{10}	Mal (m)		X_{23}	Mal (c)		X_{36}	GDP
X_{11}	Pyr (m)		X_{24}	Pyr (c)		X_{37}	GTP
X_{12}	Asp (m)		X_{26}	Asp (c)		X_{38}	FAD
X_{13}	Glu (m)		X_{26}	Glu (c)		X_{39}	$FADH_2$

TABLE I

ENTRIES OF THE CONCENTRATION VECTOR

needs 5 inputs (acetyl-CoA, NAD^+, FAD, GDP, $H_2PO_4^-$) and it gives 4 outputs (NADH, $FADH_2$, GTP, CO_2). The reaction rate vector of the CAC module is the following:

$$V_{CAC} = \begin{pmatrix} V_{CS} \cdot \frac{[OA]}{[OA]+K_{m(OA,CS)}} \cdot \frac{[AcCoA]}{[AcCoA]+K_{m(AcCoA,CS)}} \\ V_{ACON} \cdot \frac{[Cit]}{[Cit]+K_{m(Cit,ACON)}} \\ V_{ACON} \cdot \frac{[ICit]}{[ICit]+K_{m(ICit,ACON)}} \\ V_{IDH} \cdot \frac{[ICit]}{[ICit]+K_{m(ICit,IDH)}} \cdot \frac{[NAD^+]}{[NAD^+]+K_{m(NAD^+,IDH)}} \\ V_{\alpha KGDH} \cdot \frac{[\alpha KG]}{[\alpha KG]+K_{m(\alpha KG,\alpha KGDH)}} \cdot \frac{[NAD^+]}{[NAD^+]+K_{m(NAD^+,\alpha KGDH)}} \\ V_{SCS} \cdot \frac{[SucCoA]}{[SucCoA]+K_{m(SucCoA,SCS)}} \cdot \frac{[GDP]}{[GDP]+K_{m(GDP,SCS)}} \\ V_{SDH} \cdot \frac{[Suc]}{[Suc]+K_{m(Suc,SDH)}} \cdot \frac{[FAD]}{[FAD]+K_{m(FAD,SDH)}} \\ V_{FH} \cdot \frac{[Fum]}{[Fum]+K_{m(Fum,FH)}} \\ V_{FH} \cdot \frac{[Suc]}{[Suc]+K_{m(Suc,FH)}} \\ V_{MDH} \cdot \frac{[Mal]}{[Mal]+K_{m(Mal,MDH)}} \cdot \frac{[NAD^+]}{[NAD^+]+K_{m(NAD^+,MDH)}} \\ V_{MDH} \cdot \frac{[OA]}{[OA]+K_{m(OA,MDH)}} \cdot \frac{[NADH]}{[NADH]+K_{m(NADH,MDH)}} \end{pmatrix}$$

Module 2: Malate-aspartate shuttle

The malate-aspartate shuttle (MAS) contains 4 enzymes and 2 transporters. Enzymes catalyze 4 reversible reactions and transporters take place in 4 transports. The process is modeled by 14 differential equations. This module needs 2 inputs (cytoplasmic NADH and mitochondrial NAD^+) and it gives 2 outputs (cytoplasmic NAD^+ and mitochondrial NADH). The reaction rate vector of the MAS module is the following:

$$V_{MAS} = \begin{pmatrix} V_{MDH-m} \cdot \frac{[Mal_m]}{[Mal_m]+K_{m(Mal,MDH-m)}} \cdot \frac{[NAD_m^+]}{[NAD_m^+]+K_{m(NAD^+,MDH-m)}} \\ V_{MDH-m} \cdot \frac{[OA_m]}{[OA_m]+K_{m(OA,MDH-m)}} \cdot \frac{[NADH_m]}{[NADH_m]+K_{m(NADH,MDH-m)}} \\ V_{MDH-c} \cdot \frac{[Mal_c]}{[Mal_c]+K_{m(Mal,MDH-c)}} \cdot \frac{[NAD_c^+]}{[NAD_c^+]+K_{m(NAD^+,MDH-c)}} \\ V_{MDH-c} \cdot \frac{[OA_c]}{[OA_c]+K_{m(OA,MDH-c)}} \cdot \frac{[NADH_c]}{[NADH_c]+K_{m(NADH,MDH-c)}} \\ V_{ASAT-m} \cdot \frac{[OA_m]}{[OA_m]+K_{m(OA,ASAT-m)}} \cdot \frac{[Glu_m]}{[Glu_m]+K_{m(Glu,ASAT-m)}} \\ V_{ASAT-m} \cdot \frac{[Asp_m]}{[Asp_m]+K_{m(Asp,ASAT-m)}} \cdot \frac{[\alpha KG_m]}{[\alpha KG_m]+K_{m(\alpha KG,ASAT-m)}} \\ V_{ASAT-c} \cdot \frac{[OA_c]}{[OA_c]+K_{m(OA_c,ASAT-c)}} \cdot \frac{[Glu_c]}{[Glu_c]+K_{m(Glu,ASAT-c)}} \\ V_{ASAT-c} \cdot \frac{[Asp_c]}{[Asp_c]+K_{m(Asp,ASAT-c)}} \cdot \frac{[\alpha KG_c]}{[\alpha KG_c]+K_{m(\alpha KG,ASAT-c)}} \\ V_{\alpha KGT} \cdot \frac{[\alpha KG_m]}{[\alpha KG_m]+K_{m(\alpha KG_m,\alpha KGT)}} \cdot \frac{[Mal_c]}{[Mal_c]+K_{m(Mal_c,\alpha KGT)}} \\ V_{\alpha KGT} \cdot \frac{[\alpha KG_c]}{[\alpha KG_c]+K_{m(\alpha KG_c,\alpha KGT)}} \cdot \frac{[Mal_m]}{[Mal_m]+K_{m(Mal_m,\alpha KGT)}} \\ V_{AGC} \cdot \frac{[Asp_m]}{[Asp_m]+K_{m(Asp_m,AGC)}} \cdot \frac{[Glu_c]}{[Glu_c]+K_{m(Glu_c,AGC)}} \\ V_{AGC} \cdot \frac{[Asp_c]}{[Asp_c]+K_{m(Asp_c,AGC)}} \cdot \frac{[Glu_m]}{[Glu_m]+K_{m(Glu_m,AGC)}} \end{pmatrix}$$

Module 3: Citrate-pyruvate shuttle

The citrate-pyruvate shuttle (CPS) contains 8 enzymes and 3 transporters. The enzymes catalyze 6 irreversible and 2 reversible reactions and transporters take place in 6 transports. The process is modeled by 26 differential equations. This module needs 6 inputs (cytoplasmic ATP, coenzyme-A, $NADP^+$, NADH and mitochondrial ATP, NAD^+) and it gives 8 outputs (cytoplasmic NADPH, NAD^+, acetyl-CoA, ADP, CO_2 and mitochondrial ADP, NADH, CO_2). The reaction rate vector of the CPS module is the following:

$$V_{CPS} = \begin{pmatrix} V_{CS} \cdot \frac{[OA_m]}{[OA_m]+K_{m(OA,CS)}} \cdot \frac{[AcCoA_m]}{[AcCoA_m]+K_{m(AcCoA,CS)}} \\ V_{ACS} \cdot \frac{[Cit_c]}{[Cit_c]+K_{m(Cit,ACS)}} \cdot \frac{[ATP_c]}{[ATP_c]+K_{m(ATP,ACS)}} \cdot \frac{[CoA_c]}{[CoA_c]+K_{m(CoA,ACS)}} \\ V_{MDH-m} \cdot \frac{[Mal_m]}{[Mal_m]+K_{m(Mal,MDH-m)}} \cdot \frac{[NAD_m^+]}{[NAD_m^+]+K_{m(NAD^+,MDH-m)}} \\ V_{MDH-m} \cdot \frac{[OA_m]}{[OA_m]+K_{m(OA,MDH-m)}} \cdot \frac{[NADH_m]}{[NADH_m]+K_{m(NADH,MDH-m)}} \\ V_{MDH-c} \cdot \frac{[Mal_c]}{[Mal_c]+K_{m(Mal,MDH-c)}} \cdot \frac{[NAD_c^+]}{[NAD_c^+]+K_{m(NAD^+,MDH-c)}} \\ V_{MDH-c} \cdot \frac{[OA_c]}{[OA_c]+K_{m(OA,MDH-c)}} \cdot \frac{[NADH_c]}{[NADH_c]+K_{m(NADH,MDH-c)}} \\ V_{ME-m} \cdot \frac{[Mal_m]}{[Mal_m]+K_{m(Mal,ME-m)}} \cdot \frac{[NAD_m^+]}{[NAD_m^+]+K_{m(NAD^+,ME-m)}} \\ V_{ME-c} \cdot \frac{[Mal_c]}{[Mal_c]+K_{m(Mal,ME-c)}} \cdot \frac{[NADP_c^+]}{[NADP_c^+]+K_{m(NADP^+,ME-c)}} \\ V_{PDH} \cdot \frac{[Pyr_m]}{[Pyr_m]+K_{m(Pyr,PDH)}} \cdot \frac{[CoA_m]}{[CoA_m]+K_{m(CoA,PDH)}} \cdot \frac{[NAD_m^+]}{[NAD_m^+]+K_{m(NAD^+,PDH)}} \\ V_{PC} \cdot \frac{[Pyr_m]}{[Pyr_m]+K_{m(Pyr,PC)}} \cdot \frac{[CO_{2,m}]}{[CO_{2,m}]+K_{m(CO_2,PC)}} \cdot \frac{[ATP_m]}{[ATP_m]+K_{m(ATP,PC)}} \\ V_{CTP} \cdot \frac{[Cit_m]}{[Cit_m]+K_{m(Cit_m,CTP)}} \cdot \frac{[Mal_c]}{[Mal_c]+K_{m(Mal_c,CTP)}} \\ V_{CTP} \cdot \frac{[Cit_c]}{[Cit_c]+K_{m(Cit_c,CTP)}} \cdot \frac{[Mal_m]}{[Mal_m]+K_{m(Mal_m,CTP)}} \\ V_{DIC} \cdot \frac{[Mal_m]}{[Mal_m]+K_{m(Mal_m,DIC)}} \cdot \frac{[P_c]}{[P_c]+K_{m(P_c,DIC)}} \\ V_{DIC} \cdot \frac{[Mal_c]}{[Mal_c]+K_{m(Mal_c,DIC)}} \cdot \frac{[P_m]}{[P_m]+K_{m(P_m,DIC)}} \\ V_{PT} \cdot \frac{[Pyr_c]}{[Pyr_c]+K_{m(Pyr_c,PT)}} \\ V_{PT} \cdot \frac{[Pyr_m]}{[Pyr_m]+K_{m(Pyr_m,PT)}} \end{pmatrix}$$

Integrated model

The integrated model contains 16 enzymes and 5 transporters. The enzymes catalyze 10 irreversible and 6 reversible reactions and transporters take place in 10 transports. The overall model contains 39 differential equations. (Note that there are overlaps between the species and reactions of the modules.) The integrated model needs 8 inputs from the environment (cytoplasmic CoA-SH, ATP, NADH, $NADP^+$ and mitochondrial ATP, GDP, FAD, NAD^+) and it gives

10 outputs (cytoplasmic ADP, acetyl-CoA, NADPH, NAD^+, CO_2 and mitochondrial ADP, GTP, NADH, FADH2, CO_2). Naturally, the overall reaction rate vector $\bar{V}$ is the union of V_{CAC}, V_{MAS} and V_{CPS}.

The parameters of the model were either taken from the literature, or from our own laboratory measurements (Department of Medical Biochemistry, Semmelweis University). Additionally, for some enzymes we could only determine the order of magnitude of the kinetic parameters. Due to the lack of space, we cannot list the applied parameter values here, but they can be found in [11].

V. Simulation Results and Discussion

A. Implementation

The mathematical model described above, was implemented in the MATLAB environment. We have used the ode23s solver suitable for stiff problems. The initial values of the state variables (intramitochondrial and extramitochondrial concentrations) can be provided by the user, depending on the simulated metabolic status. After the calculations, the program creates several plots, that show the concentrations of the species between the initial and final time points. Each module has separate plots, which show its time-domain behaviour.

B. Simulation results

In this subsection, we present simulation results and the corresponding brief discussion for the individual modules, and finally for the integrated model. The initial concentrations are given in mmol.

Module 1: Citric acid cycle The initial values were 0.5 (acetyl-CoA, oxaloacetate, NAD, FAD, GDP, $H_2PO_4^-$, CoA-SH) or zero (other components). We supply the system in every cycle with acetyl-CoA, NAD^+, FAD, GDP, $H_2PO_4^-$ (1:3:1:1:1 ratio). In the results we can see, that the components of the citric acid cycle reach steady state, except for α-ketoglutarate, malate and fumarate (Figure 5). Later we will give explanation for that using the integrated model.

Module 2: Malate-aspartate shuttle The initial values in mitochondrion were the following: oxaloacetate is 0.5, α-ketoglutarate, malate and NADH are zero, glutamate and aspartate are 0.25, and NAD^+ is 0.5. Initial values in cytoplasm are 0.2 except NAD^+ (0) and NADH (0.5). We supply the system in every cycle with mitochondrial NAD^+ and cytosolic NADH (1:1 ratio) and we eliminate the outputs (mitochondrial NADH and cytosolic NAD^+, 1:1 ratio). The results show that the components of the malate-aspartate shuttle reach steady state both in the mitochodrion (Figure 6) and in the cytoplasm (Figure 7). This simulation shows that the sub-model can produce NAD^+/NADH equilibrium status between the two sides of the inner membrane.

Module 3: Citrate-pyruvate shuttle The initial values in the matrix were the following: acetyl-CoA, CoA-SH, oxaloacetate, pyruvate, ATP, $H_2PO_4^-$ and NAD are 0.5, and other

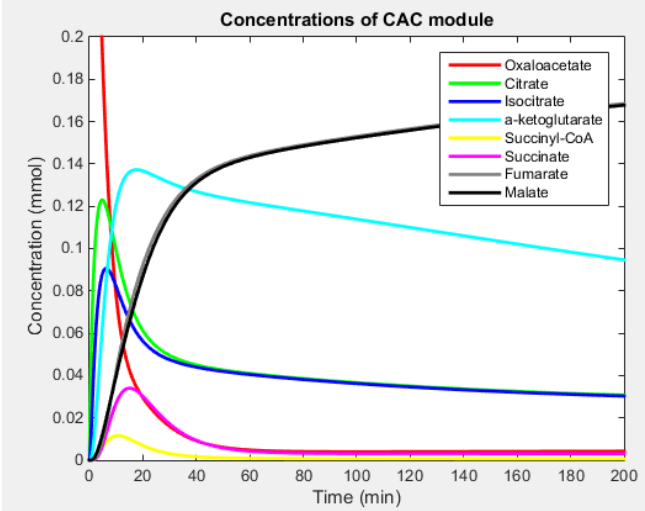

Fig. 5. Concentrations of citric acid cycle molecules

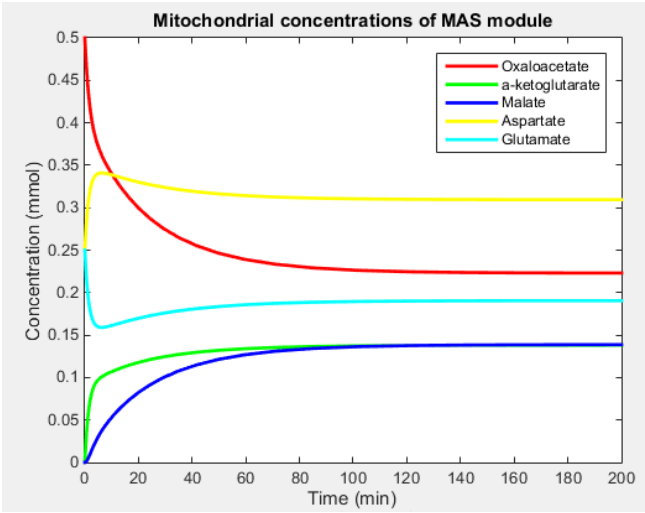

Fig. 6. Mitochondrial concentrations of MAS

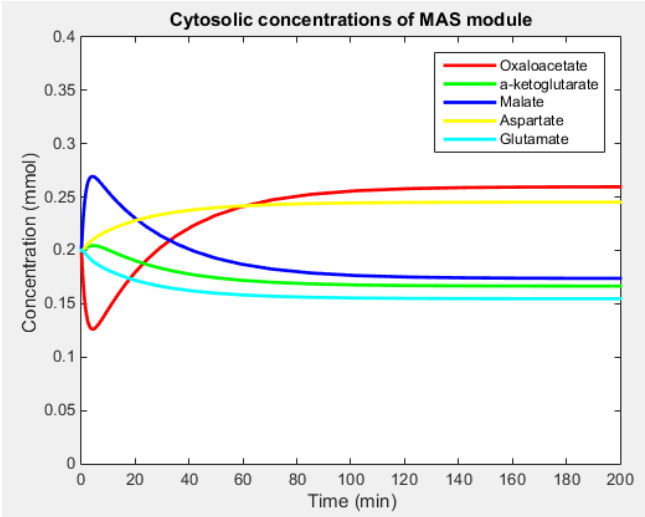

Fig. 7. Cytosolic concentrations of MAS

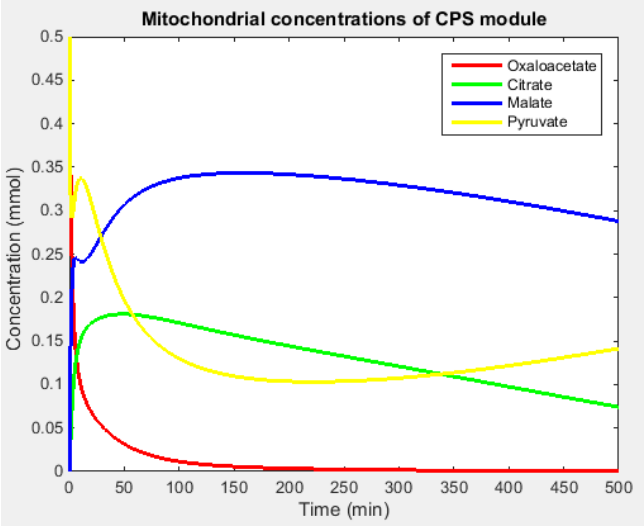

Fig. 8. Mitochondrial concentrations of CPS

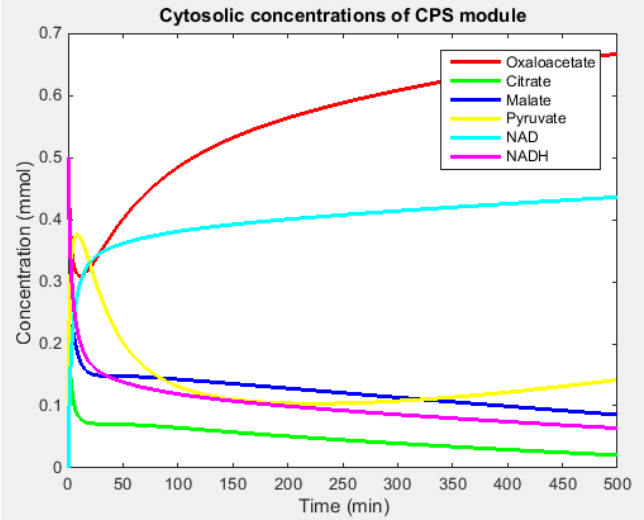

Fig. 9. Cytosolic concentrations of CPS

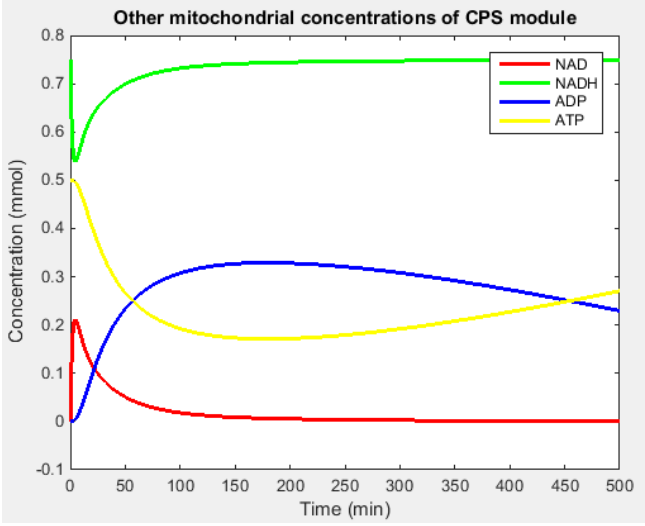

Fig. 10. Other mitochondrial components of CPS module

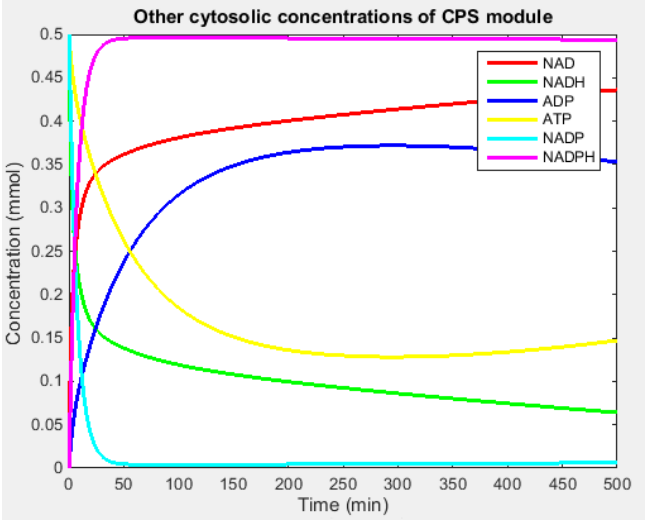

Fig. 11. Other cytosolic components of CPS module

components were zero. Initial values in the cytoplasm: CoA-SH, NADH, NADP, ATP and $H_2PO_4^-$ are 0.5, oxaloacetate, citrate and malate are 0.2, and other components are zero. We supply the system in every cycle with cytoplasmic coenzyme A, ATP, NADH, $NADP^+$ and mitochondrial ATP, NAD^+. We eliminate cytoplasmic acetyl-CoA, ADP, NAD^+, NADPH, CO_2 and mitochondrial NADH and ADP (1:1 ratio). It is clear from the simulations that this module needs further improvement: The components don't reach appropriate steady state in the matrix (Figure 8) and in the cytoplasm (Figure 9), because in every cycle the system loses 3 carbon atoms (two with acetyl-CoA, and one with CO_2). In the mitochondrion NAD^+-NADH and ADP-ATP (Figure 10), in the cytoplasm NAD^+-NADH, $NADP^+$-NADPH and ADP-ATP (Figure 11) show reciprocal behavior, because these molecules change just their redox or phosphorylation status.

The integrated model

The initial values in the matrix were same as in the previous simulations: acetyl-CoA, CoA-SH, oxaloacetate, pyruvate, NAD^+, FAD, GDP, ATP and $H_2PO_4^-$ are 0.5, aspartate and glutamate are 0.25, and other concentrations are zero. Initial values in cytoplasm: CoA-SH, NADH, $NADP^+$, ATP and $H_2PO_4^-$ are 0.5, oxaloacetate, citrate, α-ketoglutarate, malate, aspartete and glutamate are 0.2, and other components are zero. We supply the system in every cycle with cytoplasmic coenzyme A, ATP, NADH, $NADP^+$ and mitochondrial ATP, GDP, FAD and NAD (1:1:1:3 ratio). We eliminate cytoplasmic acetyl-CoA, ADP, NAD^+, NADPH, CO_2 and mitochondrial ADP, GTP, $FADH_2$, NADH, CO_2 (1:1:1:3:2 ratio). The results show that the dynamical behavior of the integrated model differs at several points from the individual sub-models. If we "feed" the mitochondria (we give extra malate in the extramitochondrial space with a ration of 1.37), then the model reaches steady state.

We make the first comparison between the components of the citric acid cycle. The integrated model shows that all of the molecules reach steady state, because it is not an isolated system any more. Most of the components have at least one alternative pathway, which they can use, and due to this we can see equilibriation by these molecules (Figure 12).

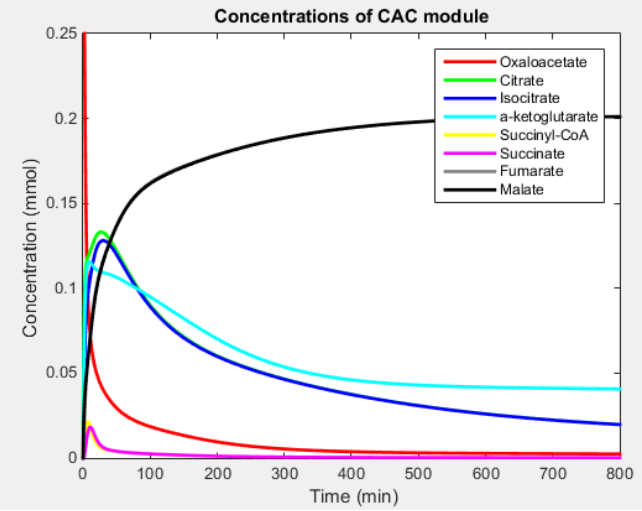

Fig. 12. Concentrations of citric acid cycle molecules

The second comparison is between the mitochondrial components of the malate-aspartate shuttle. This module connects to the citric acid cycle via mitochondrial malate, oxaloacetate, α-ketoglutarate, NAD^+ and NADH, because these molecules take part in both processes. The results show that the connection modifies the operation of the malate-aspartate shuttle. NADH can be oxidized in the electron transport chain (we eliminate that) and decreases its amount. Due to this the malate + $NAD^+ \rightleftharpoons$ oxaloacetate + NADH reaction becomes faster in the right direction, and this implies that the amount of malate is lower than in the individual sub-model. In another case, when the intramitochondrial malate is low, the α-ketoglutarate transporter functions rapidly. It carries more malate from the cytoplasm to the mitochondrial matrix and carries α-ketoglutarate to reverse direction. Due to this the intramitochondrial α-ketoglutarate decreases. In the integrated model, aspartate and glutamate concentrations in the matrix show reciprocal behavior because of the aspartate aminotransferase transport (Figure 13).

The third comparison is when we compare the cytoplasmic concentrations, we recognize that they are substantially different. The amount of malate decreases, because of the α-ketoglutarate transporter as we mentioned before. Due to this malate + $NAD^+ \rightleftharpoons$ oxaloacetate + NADH reaction goes to reverse direction, which results that the concentration of oxaloacetate decreases. Because of this the system goes towards the restoration of the equilibrium state, produces oxaloacetate (and glutamate) from aspartate and (transported) α-ketoglutarate. Due to this, additional concentrations change: malate and glutamate increases, α-ketoglutarate, oxaloacetate and aspartate decrease and every

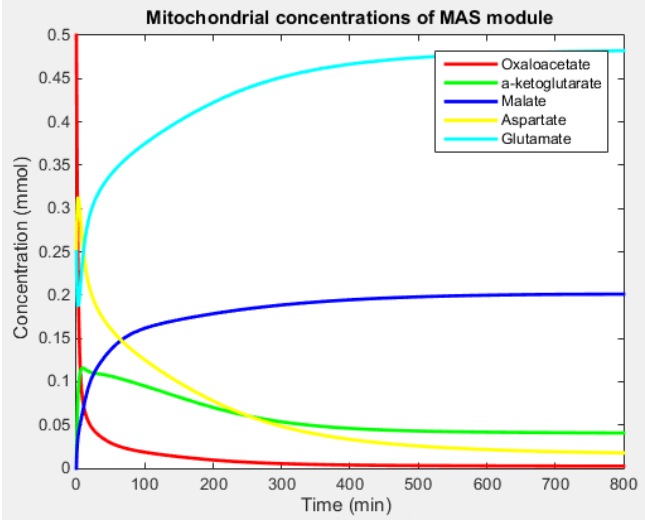

Fig. 13. Concentrations of MAS molecules in the matrix

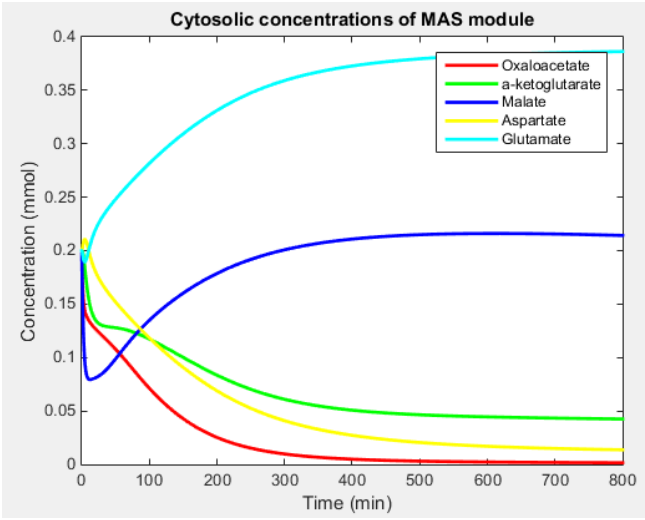

Fig. 14. Concentrations of MAS molecules in the cytoplasm

substrate reach steady state (Figure 14).

The fourth comparison is between the mitochondrial components of the citrate-pyruvate shuttle. This module connects to the citric acid cycle via mitochondrial citrate, malate, oxaloacetate, acetyl-CoA, coenzyme A, NAD^+ and NADH. These molecules take part in both processes. Because of the concentration differences, intramitochondrial malate reaches the steady state, and its concentration is higher in the integrated model, because we feed the mitochondrion. The citrate decrease rate is higher in the integrated model than in the individual module, because it has two potential elimination pathways. Oxaloacetate decrease has quite similar kinetics in the individual module and the integrated system. Malic enzyme can produce extramitochondrial pyruvate form malate, because of this reaction if we feed the mitochondria with malate, that increases pyruvate, which is equilibrated matrix concentration via pyruvate transporter (Figure 15).

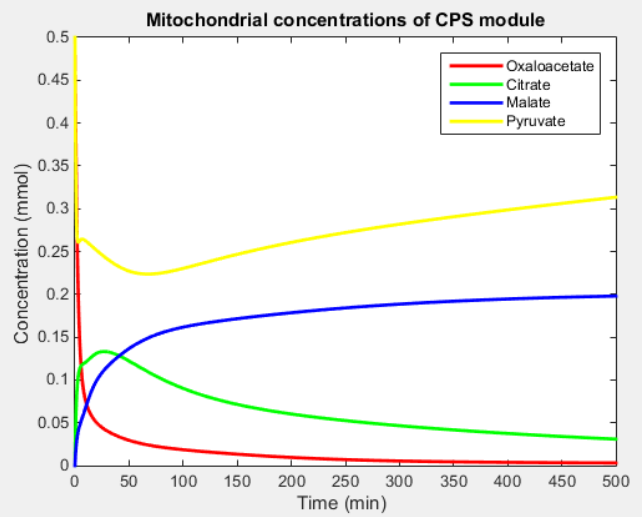

Fig. 15. Concentrations of CPS molecules in the matrix

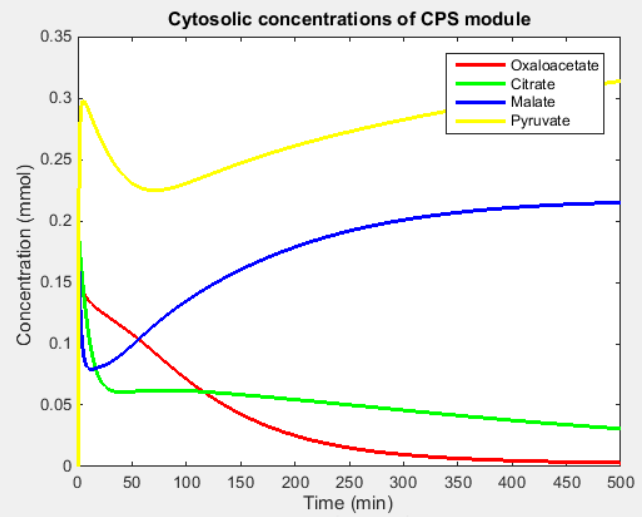

Fig. 16. Concentrations of CPS molecules in the cytoplasm

The last comparison is about the cytoplasmic concentration of the citrate-pyruvate shuttle's molecules. Oxaloacetate in the integrated model can react in the MAS module and can be eliminated. Malate concentration is higher as we mentioned in the fourth comparison. The concentration of citrate is lower than in the individual module since the intramitochondrial concentration of citrate is lower due to the aconitase reaction, and less intramitochondrial citrate leads slower transport via citrate transporter, which leads less extramitochondrial citrate (Figure 16).

VI. CONCLUSIONS

In this work, we introduced a dynamic model for describing the dynamics of key quantities in mitochondrial metabolism. This kinetic system was written in the form of 39 nonlinear ordinary differential equations assuming Michaelis-Menten kinetics. Initially, the sub-models of the three subsystems were developed and tested, and then these modules were integrated into a unified dynamical model. The main difference of the model compared to results in the literature known by the authors is that no constant assumption was made on the described species concentrations (e.g. the extensive model in [8] describes 15 enzymes and 5 transporters and uses 39 concentrations of metabolites out of which 15 are constant). In this way, it is theoretically possible to study the dynamical interplay between all described species.

Simulations show that the obtained results are qualitatively correct for our expectations. However, there are important inaccuracies which necessitate further work. Additional laboratory measurements are in progress to determine kinetic parameters about which we have incomplete knowledge. Besides further model development, future work will also be focused on the sensitivity and identifiability analysis of the system to support experiment design. An important planned application of the model is the dynamical description and related study of pathological processes such as ischaemia.

REFERENCES

[1] Tretter, L. and Adam-Vizi, V. (2004). Generation of reactive oxygen species in the reaction catalyzed by alpha-ketoglutarate dehydrogenase. *The Journal of Neuroscience*, 24(36), 7771–8.

[2] Adam-Vizi, V. and Tretter, L. (2013). The role of mitochondrial dehydrogenases in the generation of oxidative stress. *Neurochemistry International*, 62(5), 757–63.

[3] Tretter, L., Horvath, G., Hőgyesi, A., Essek, F., and Adam-Vizi, V. (2014). Enhanced hydrogen peroxide generation accompanies the beneficial bioenergetic effects of methylene blue in isolated brain mitochondria. *Free Radicical Biology & Medicine*, 77, 317–30.

[4] Ambrus, A., Nemeria, N., Torocsik, B., Tretter, L., Nilsson, M., Jordan, F., and Adam-Vizi, V. (2015). Formation of reactive oxygen species by human and bacterial pyruvate and 2-oxoglutarate dehydrogenase multienzyme complexes reconstituted from recombinant components. *Free Radicical Biology & Medicine*, 89, 642–50.

[5] Wu, F., Yang, F., Vinnakota, K., and Beard, D. (2007). Computer modeling of mitochondrial tricarboxylic acid cycle, oxidative phosphorylation, metabolite transport, and electrophysiology. *The Journal of Biological Chemistry*, 282(34), 24525–37.

[6] Nazaret, C., Heiske, M., Thurley, K., and Mazat, J. (2009). Mitochondrial energetic metabolism: a simplified model of tca cycle with atp production. *The Journal of Theoretical Biology*, 258(3), 455–64.

[7] Korla, K. and Mitra, C. (2014). Modelling the krebs cycle and oxidative phosphorylation. *Journal of Biomolecular Structure and Dynamics*, 32, 242–256.

[8] Korla, K., Vadlakonda, L., and Mitra, C. (2015). Kinetic simulation of malate-aspartate and citrate-pyruvate shuttles in association with krebs cycle. *Journal of Biomolecular Structure and Dynamics*, 33(11), 2390–403.

[9] Nelson, D.L. and Cox, M.M. (2012). *Lehninger Principles of Biochemistry*. WH Freeman, 6 edition.

[10] Korla, K. and Mitra, CK. (2014). Kinetic modelling of coupled transport across biological membranes. *Indian Journal of Biophysics*, 51(2), 93–9.

[11] Sváb, G. (2018). Modeling of mitochondrial metabolism. *MSc thesis*, http://www.eregistrator.hu/drsvabgergely/Gergely_Svab_2017.pdf